Supplemental Information

Engineered enzymatic cascade converts diols to amino alcohols

Hannah R. Valentino[1], Liangyu Qian[1], Jerry M. Parks[1], Erin E. Drufva[1], Ada Sedova[1], Pankti S. Mehta[2], Mary P. Watson[2], Richard J. Giannone[1], Stephanie S. Galanie[1,‡], and Joshua K. Michener[1,†]

[1]Biosciences Division, Oak Ridge National Laboratory, Oak Ridge, TN 37831, USA;
[2]Department of Chemistry and Biochemistry, University of Delaware, Newark, Delaware 19716, USA

[‡]Present address: Merck

[†]To whom correspondence should be addressed: michenerjk@ornl.gov

Supplementary Figures

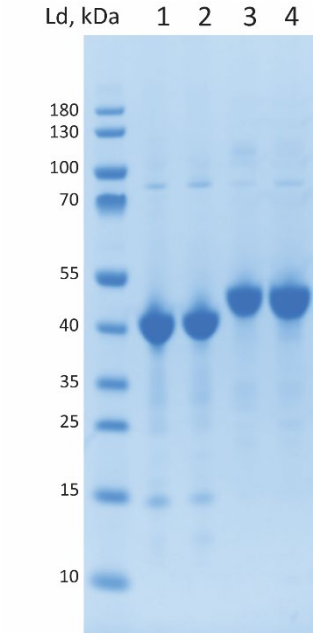

Supplemental Figure 1: Representative purification of ADH, AmDH, and AmDH+. The molecular weight ladder used was PageRuler Prestained Protein Ladder (Thermo Scientific). Each well contains purified enzyme of 1) ADH, 2) Mutant ADH (not discussed), 3) AmDH, and 4) AmDH+.

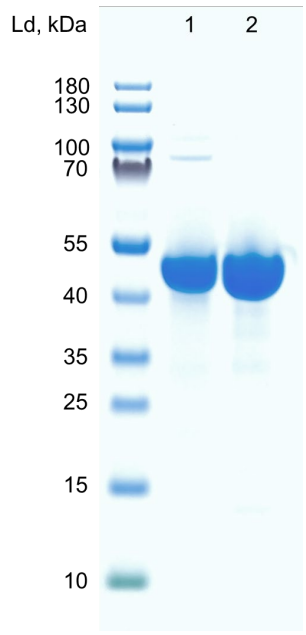

Supplemental Figure 2: Representative purification of AmDH+ and AmDH+/L146V. The molecular weight ladder used was PageRuler Prestained Protein Ladder (Thermo Scientific). Each well contains purified product of 1) AmDH+ and 2) AmDH+/L146V.

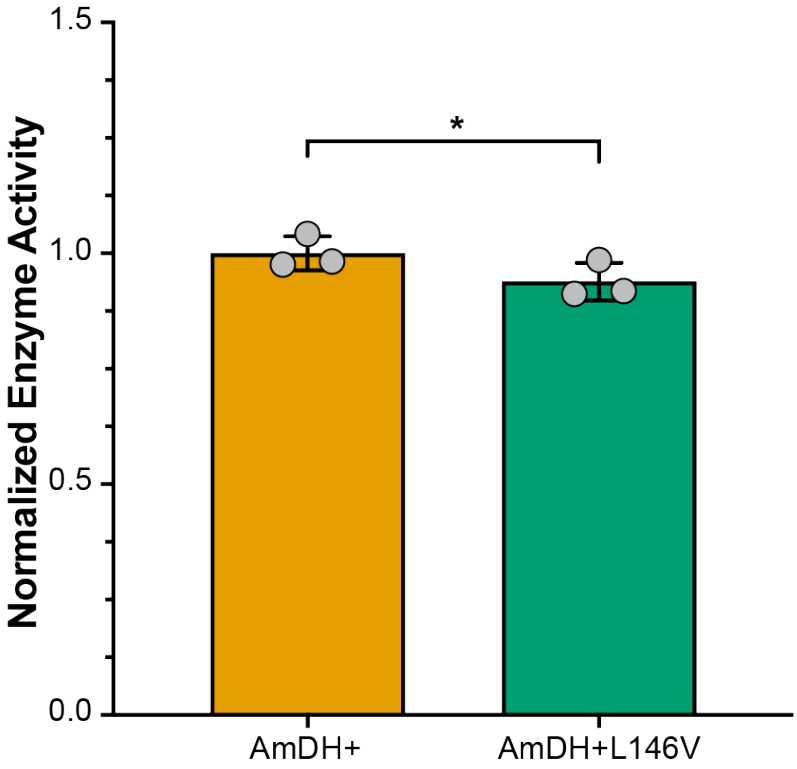

Supplemental Figure 3: Activity of AmDH+ L146V revertant. Activity comparison of purified AmDH+ and L146V revertant for conversion of 6-hydroxyhexanal to 6-aminohexanol. Assay conditions were 0.7 M NH_4Cl (pH 8), 2.5 mM 6-hydroxyhexanal, 0.7 mM NADH, 10% DMSO, and 2 µM enzyme at 30 °C. Error bars represent the standard deviation of the normalized data. p value was obtained by doing a paired t-test. *: $p < 0.05$.

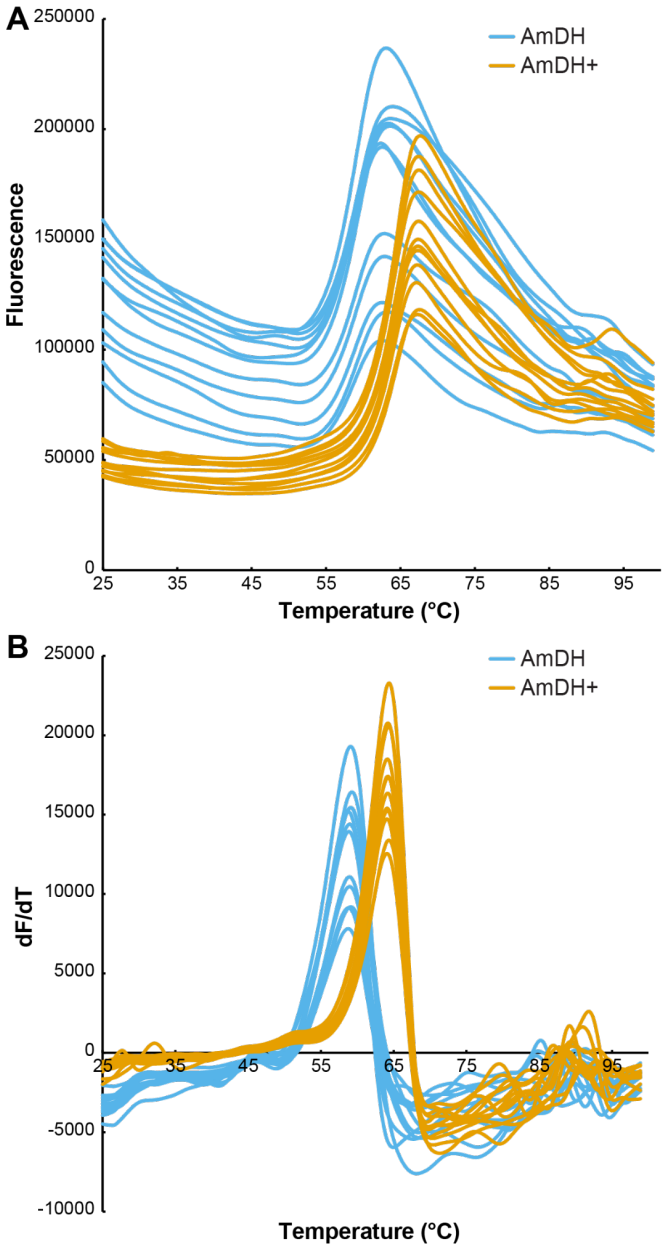

Supplemental Figure 4: PTSA melting curves for AmDH and AmDH+. Purified enzyme was heated through a temperature gradient in the presence of a hydrophobic dye. Protein unfolding was monitored fluorimetrically using a quantitative thermocycler. The melting temperature was calculated with the Thermo Fisher Protein Thermal Shift Software using the derivative method to determine the inflection point of the fluorescence curve. Twelve replicates are shown for each enzyme. (A) Fluorescence vs. temperature. (B) Derivative plot of the change in fluorescence (F) vs. temperature.

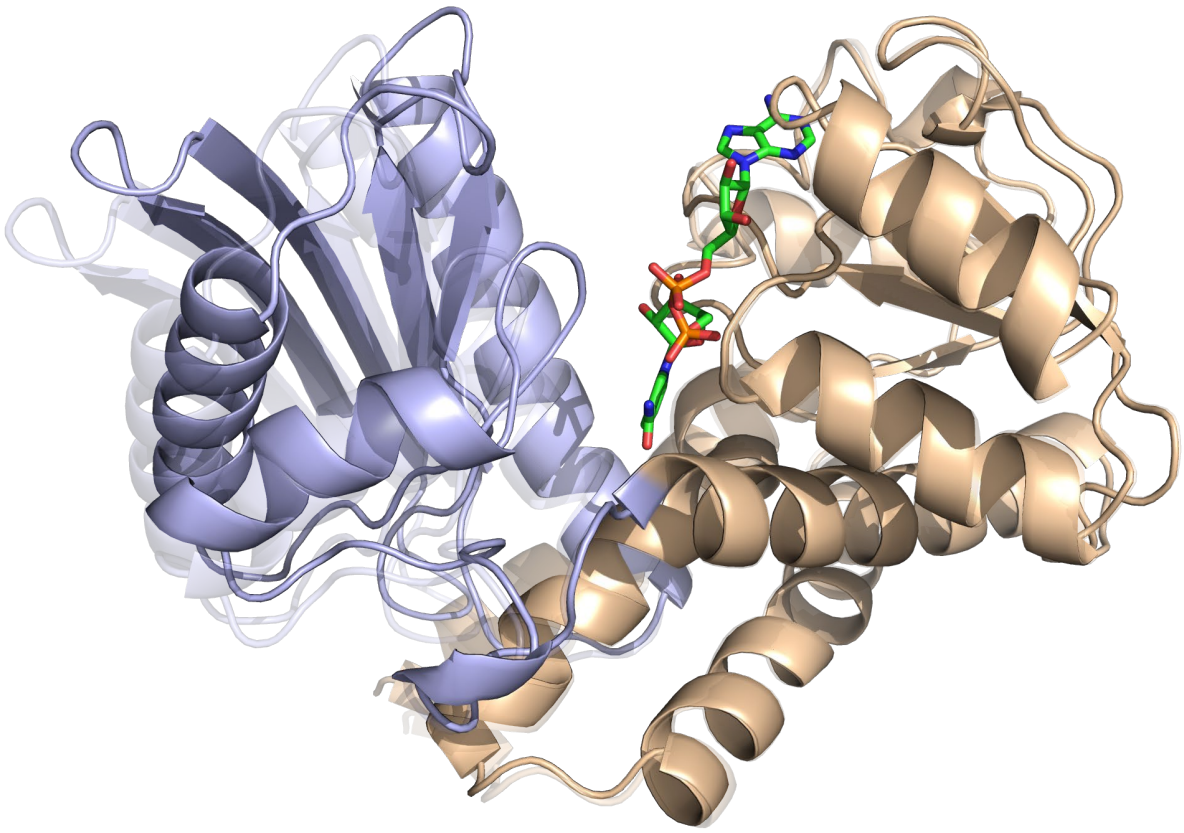

Supplemental Figure 5: Structural alignment of the AmDH and AmDH+ models. To show the relative positions of the two domains in each protein, only the cofactor binding domains (Domain 2) were aligned. The parent model is shown in semi-transparent cartoon representation. Colors: Domain 1, light blue; Domain 2, wheat. Regions at the N- and C-termini with low model confidence are not shown.

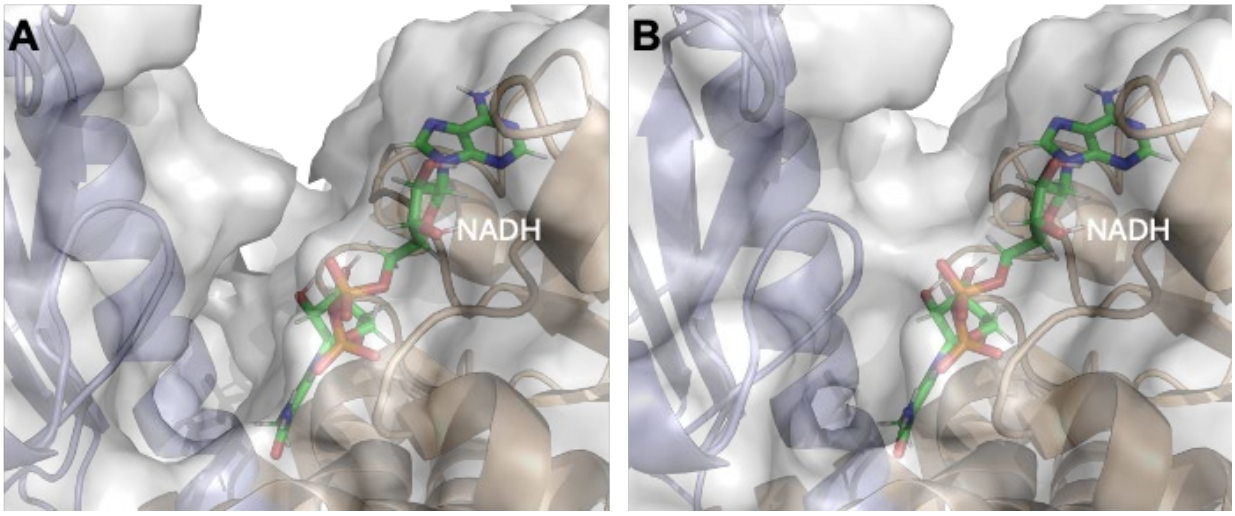

Supplemental Figure 6: Surface representation of the AmDH active site region. The active site of AmDH (A) is larger and more open than that of AmDH+ (B). Colors: Domain 1, light blue; Domain 2, wheat. NADH is shown in green sticks.

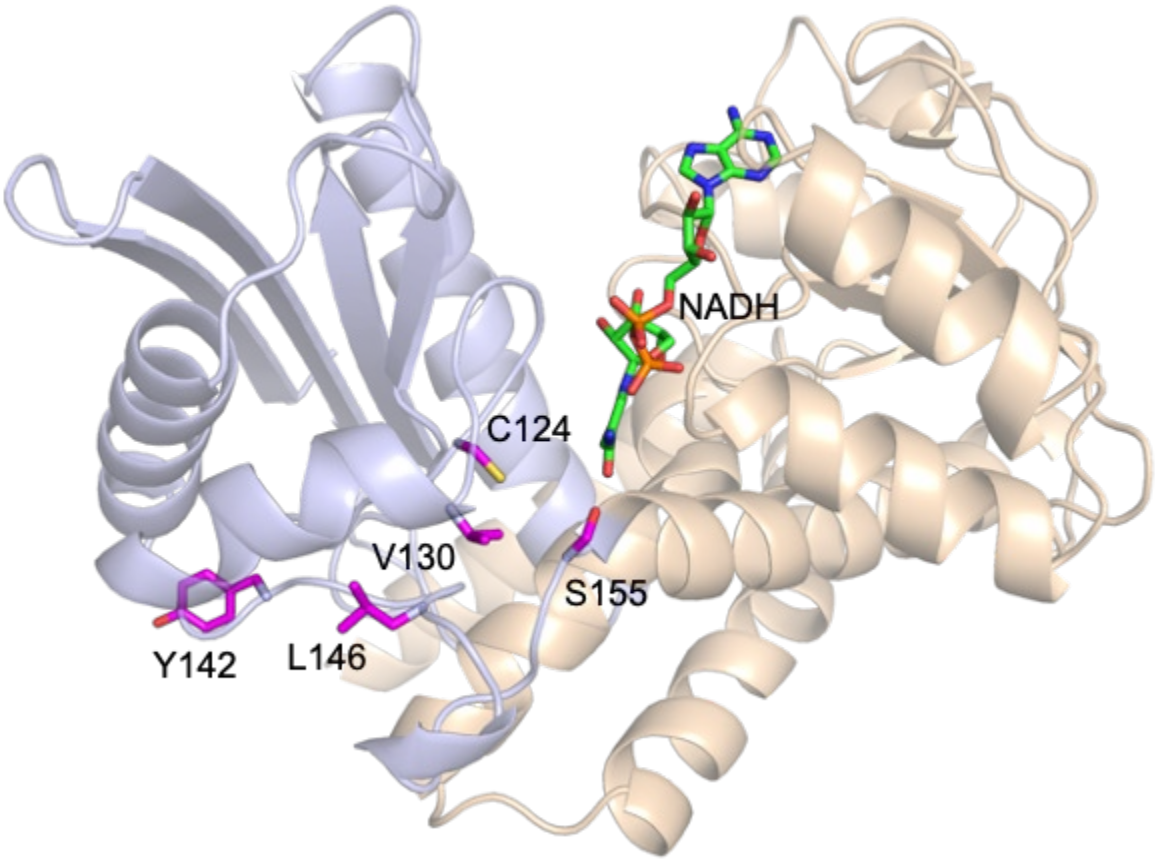

Supplemental Figure 7: Mutation sites in AmDH+. Colors: Domain 1, light blue; Domain 2, wheat. Mutated residues are labeled and shown in magenta sticks; NADH is shown in green sticks.

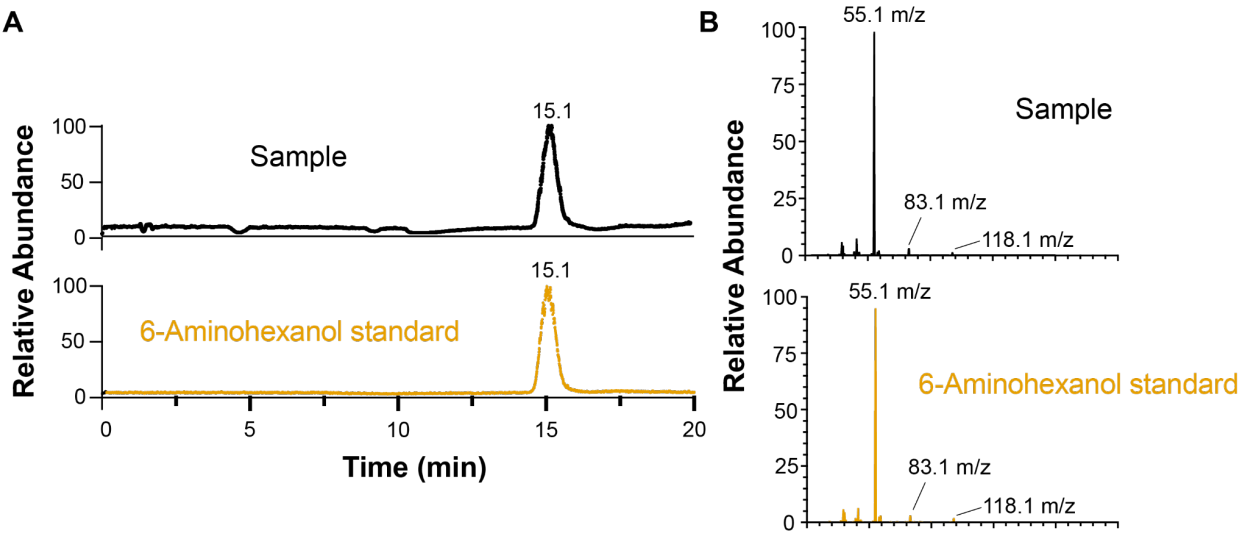

Supplemental Figure 8: Mass spectrum of enzymatically-synthesized 6-aminohexanol. 6-Aminohexanol measured in sample (top) versus standard (bottom) showing (A) retention time and (B) MS/MS fragmentation profiles. 6-Aminohexanol was fragmented using a collision energy of 20V. The main fragments of the 6-aminohexanol standard (orange) match with those observed in the sample at the peak eluting around 15.1 min (black).

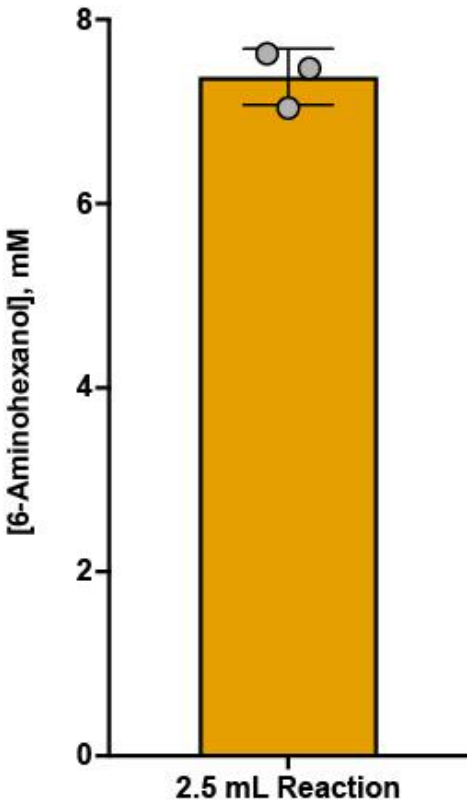

Supplemental Figure 9: 6-Aminohexanol production by engineered enzyme cascade. Purified ADH (10 μM) and AmDH+ (20 μM) were incubated with 50 mM of 1,6-hexanediol for 24h. The production yield (~7 mM) was comparable to that observed in the small-scale experiments shown in Figure 6. 6-Aminohexanol formation was monitored by LC-MS. Error bars show one standard deviation, calculated from three biological replicates.

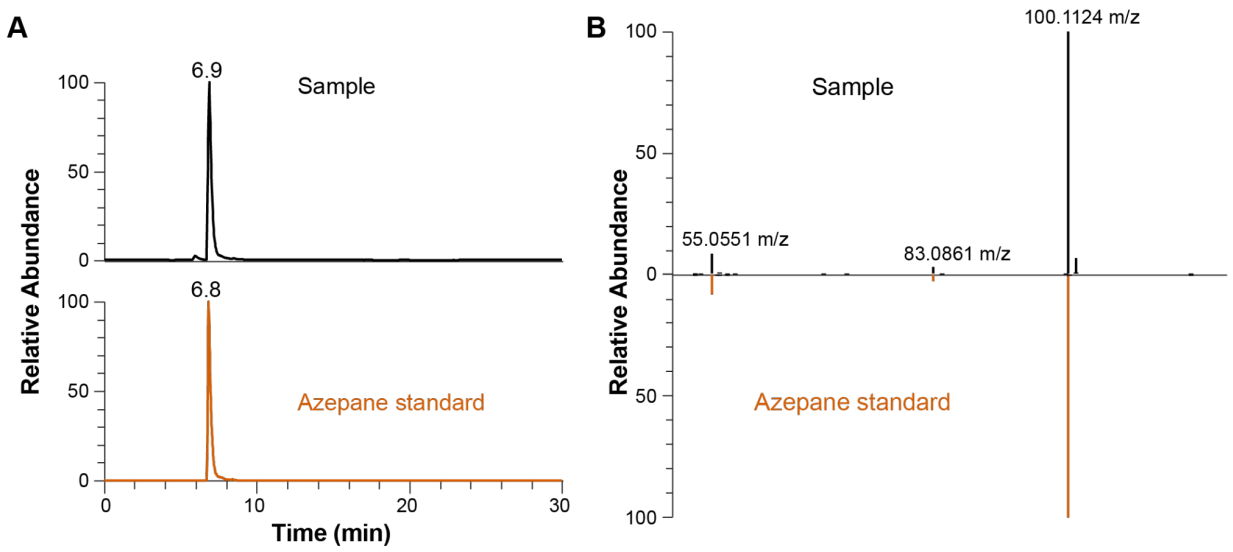

Supplemental Figure 10: Mass spectrum of enzymatically-synthesized azepane. Azepane measured in sample (top) versus standard (bottom) showing (A) retention time and (B) MS/MS fragmentation profiles via parallel reaction monitoring. Azepane was fragmented by HCD using stepped normalized collision energy of 30/35/40 (averaged). Main fragments of azepane standard (labeled) match with those observed in the sample at the peak eluting around 6.8 to 6.9 min.

Supplementary Tables

Supplemental Table 1: Mass spectrometry parameters

Condition*	1	2
Gas temp, °C	300	65
Gas flow, mL/min	11	11
Nebulizer, psi	35	35
Sheath gas temperature, °C	350	350
Sheath gas flow, l/min	11	11
Capillary, V	3500	3500
Nozzle voltage, V	2000	2000

*Condition 2 was used for detection of pyrrolidine and 4-aminobutanol, while condition 1 was used for all other compounds

Supplemental Table 2: MRM monitoring ions

Compound		Precursor, m/z	Product Ion, m/z	Fragmentor, V	Collision Energy	CAV	Polarity
7-aminoheptanol	Quantifier	132.1	69.1	90	12	6	positive
	Qualifier	132.1	97.1	90	8	6	positive
6-aminohexanol	Quantifier	118.1	83.1	70	8	4	positive
	Qualifier	118.1	55.1	70	20	4	positive
5-aminopentanol	Quantifier	104.1	86.7	70	8	4	positive
	Qualifier	104.1	41.2	70	20	4	positive
4-aminobutanol	Quantifier	90.1	73.1	30	8	0	positive
	Qualifier	90.1	55.1	30	16	0	positive
Azocane	Quantifier	114.1	55.1	94	20	6	positive
	Qualifier	114.1	69.1	94	16	6	positive
Hexamethyleneimine (Azepane)	Quantifier	100.1	55.1	70	20	8	positive
	Qualifier	100.1	83.1	70	12	8	positive
Piperidine	Quantifier	86.1	69.1	70	16	7	positive
	Qualifier	86.1	41.2	70	20	7	positive
Pyrrolidine	Quantifier	72.1	55.1	30	20	5	positive
	Qualifier	72.1	44.2	30	20	5	positive
Amylamine	Quantifier	88.1	71.1	70	8	4	positive
	Qualifier	88.1	43.2	70	16	4	positive
1,6-hexane diamine	Quantifier	117.1	100.1	70	8	5	positive
	Qualifier	117.1	55.1	70	20	5	positive
1,5-pentane diamine	Quantifier	103.1	86.1	70	8	5	positive
	Qualifier	103.1	41.2	70	20	5	positive
1,7-heptane diamine	Quantifier	131.2	69.1	70	8	6	positive
	Qualifier	131.2	55.1	70	8	6	positive

Supplemental Table 3: Alkanolamine and cyclic amine production with the parental alcohol and amine dehydrogenase cascade. Reaction conditions were 50 mM substrate, 1 mM NAD+, 10 μM alcohol dehydrogenase, and 10 μM amine dehydrogenase in 2 M ammonium chloride (pH 8) at 30 ºC. Reactions were quenched at 24 hours and products measured by LC-MS/MS.

substrate	alkanolamine		cyclic amine	
	product	concentration, μM	product	concentration, μM
1,4-butanediol	4-aminobutanol	300 ± 100	pyrrolidine	N.D.[a]
1,5-pentanediol	5-aminopentanol	60 ± 4	piperidine	N.D.
1,6-hexanediol	6-aminohexanol	250 ± 50	azepane	N.D.
1,7-heptanediol	7-aminoheptanol	50 ± 8	azocane	N.D.
4-aminobutanol	N.A.[b]		pyrrolidine	N.D.
5-aminopentanol	N.A.		piperidine	900 ± 100
6-aminohexanol	N.A.		azepane	2300 ± 30
7-aminoheptanol	N.A.		azocane	20 ± 2

[a] N.D. represents not detectable
[b] N.A. represents not applicable

Supplemental Table 4: Steady-state kinetic parameters of ADH with diol and alkanolamine substrates. Conditions were 0.5 μM enzyme, 10 mM NAD+, and 0.5-500 mM substrate in 2 M 2 M NH_4Cl (pH 8) at 30 ℃.

variable substrate	k_{cat}, s^{-1}	K_m, mM	k_{cat}/K_m , M^{-1} s^{-1}
1,4-butane diol	2 ± 0.1	76 ± 9	26 ± 3
1,5-pentane diol	0.8 ± 0.04	50 ± 4	16 ± 2
1,6-hexane diol	1.04 ± 0.01	60 ± 2	17 ± 1
1,7-heptane diol	0.1 ± 0.01	30 ± 6	3.3 ± 0.7
4-aminobutanol		N.D.	
5-aminopentanol	0.7 ± 0.2	500 ± 100	1 ± 0.08
6-aminohexanol	1 ± 0.1	600 ± 80	1.6 ± 0.01

Supplemental Table 5: Steady-state kinetic parameters of AmDH and AmDH+ with hexanal and 6-hydroxyhexanal. Conditions for the 6-hydroxyhexanal substrate variation were 2 M NH_4Cl pH 8, 10% DMSO, 10 μM AmDH or 2 μM AmDH+, 0.7 mM NADH, and varying concentration of 6-hydroxyhexanal from 0.1-5 mM. Conditions for hexanal variation were 2 M NH_4Cl (pH 8), 10% DMSO, 1 μM AmDH, 0.7 mM NADH, and varying concentrations of hexanal from 0.05-2.5 mM.

Enzyme	Varied substrate	k_{cat} s^{-1}	K_M mM	k_{cat}/K_M M^{-1} s^{-1}
AmDH	6-hydroxyhexanal	0.007 ± 0.002	1.1 ± 0.4	6 ± 3
AmDH	hexanal	0.13 ± 0.01	0.4 ± 0.07	300 ± 30
AmDH+	6-hydroxyhexanal	0.15 ± 0.02	2.6 ± 0.6	60 ± 15

Supplemental Table 6: AmDH mutant screening. Enzymes were assayed in lysate containing 0.3 mM NADH, 2.5 mM 6-hydroxyhexanal, 10% DMSO, and 20% cell lysate in 2 M NH_4Cl (pH 8) at 30 ℃ for 10 min and compared to parental AmDH.

Mutations	Fold improvement over parent
T124C/M130V/C142Y/V146L/N155S	11.7 ± 0.6
T124C/C142Y/N155S/P158R	6.4 ± 1.4
T124C/C142Y/N155S/P158R	7.6 ± 2.2
T124C/C142Y/N155S	6.0 ± 1.4
T124C/C142Y/N155S/P158L	7.6 ± 2.7
T124C/C142Y/N155S	7.8 ± 0.5
T124C/C142Y/N155S/P158L	7.2 ± 1.0

Supplementary Table 7: Alkanolamine and cyclic amine production from diols. Reaction conditions were 50 mM substrate, 1 mM NAD+, 10 μM alcohol dehydrogenase, and 10 μM amine dehydrogenase in 2 M NH_4Cl (pH 8) at 45 ºC. Reactions were quenched at 24 hours and products measured by LC-MS/MS.

substrate	enzyme combination	alkanolamine, μM	cyclic amine, μM
1,4-butanediol	ADH/AmDH	N.D.[a]	N.D.
	ADH/AmDH+	60 ± 10	N.D.
1,5-pentanediol	ADH/AmDH	100 ± 7	N.D.
	ADH/AmDH+	900 ± 30	40 ± 10
1,6-hexanediol	ADH/AmDH	900 ± 50	5 ± 1
	ADH/AmDH+	7000 ± 200	70 ± 5
1,7-heptane diol	ADH/AmDH	100 ± 60	N.D.
	ADH/AmDH+	300 ± 20	N.D.

[a] N.D. represents not detectable

Supplementary Table 8: Cyclic amine production from alkanolamines. Reaction conditions were 50 mM substrate, 1 mM NAD+, 10 μM alcohol dehydrogenase, and 10 μM amine dehydrogenase in 2 M NH_4Cl pH 8 at 45 ºC. Reactions were quenched at 5 and 24 hours and products measured by LC-MS/MS.

substrate	enzyme combination	cyclic amine, 5h, μM	cyclic amine, 24 h μM
4-aminobutanol	ADH/AmDH	20 ± 7	20 ± 7
	ADH/AmDH+	51 ± 5	140 ± 30
5-aminopentanol	ADH/AmDH	200 ± 70	2000 ± 150
	ADH/AmDH+	4000 ± 400	5000 ± 700
6-aminohexanol	ADH/AmDH	200 ± 90	1400 ± 30
	ADH/AmDH+	4000 ± 40	3100 ± 300
7-aminoheptanol	ADH/AmDH	9 ± 4	200 ± 60
	ADH/AmDH+	130 ± 30	160 ± 50

Supplemental Table 9: Primers used in this study

Name	Use	Sequence
A32 FWD	Site-saturation mutagenesis	5'-ACGATCCGNDTACAGGACTAAG-3’
A32 REV	Site-saturation mutagenesis	5'-TGCAAAAAACAACTTGTTCATGTTCAGAC-3’
L50 FWD	Site-saturation mutagenesis	5'-ACACTCGGACCTGCGNDTGG-3’
L50 REV	Site-saturation mutagenesis	5'-GGTGTCATGAATAGCGATAATGGCCCTTAGTC-3’
G123 FWD	Site-saturation mutagenesis	5'-GGCCGTTTCTATACANDTACTGATATGGG-3’
G123 REV	Site-saturation mutagenesis	5'-GCCAAGCGAATCAACAAATTGGC-3’
T124 FWD	Site-saturation mutagenesis	5'-GCCGTTTCTATACAGGTNDTGATATGGG-3’
T124 REV	Site-saturation mutagenesis	5'-CGCCAAGCGAATCAACAAATTGGC-3’
I134 FWD	Site-saturation mutagenesis	5'-GGAAGATTTCNDTCACGCCATGAAAG-3’
I134 REV	Site-saturation mutagenesis	5'-ATATTCGTTCCCATATCAGTACCTGTATAGAAACGG-3’
T140 FWD	Site-saturation mutagenesis	5'-CCATGAAAGAANDTAACTGCATTGTTGGGG-3’
T140 REV	Site-saturation mutagenesis	5'-CGTGAATGAAATCTTCCATATTCGTTCCCATATCAGTACC-3’
V144 FWD	Site-saturation mutagenesis	5'-GAAACAAACTGCATTNDTGGGGTGCC-3’

V144 REV	Site-saturation mutagenesis	5'-TTTCATGGCGTGAATGAAATCTTCCATATTCGTTCCC-3’
C301 FWD	Site-saturation mutagenesis	5'-GGCGGCNDTATCAACGTCG-3’
C301 REV	Site-saturation mutagenesis	5'-GGCGTTGATCACATAATCCGGG-3’
I302 FWD	Site-saturation mutagenesis	5'-GGCGGCTGCNDTAACGTCG-3’
I302 REV	Site-saturation mutagenesis	5'-GGCGTTGATCACATAATCCGGGG-3’
N303 FWD	Site-saturation mutagenesis	5'-GCGGCTGCATCNDTGTCGC-3’
N303 REV	Site-saturation mutagenesis	5'-CGGCGTTGATCACATAATCCGGGG-3’
V304 FWD	Site-saturation mutagenesis	5'-GCCGGCGTTGATCACATAATCCGGGG-3’
V304 REV	Site-saturation mutagenesis	5'-GCCGGCGTTGATCACATAATCCGGGG-3’
E307 FWD	Site-saturation mutagenesis	5'-CAACGTCGCGGACNDTCTGTACGGCTACAATCG-3’
E307 REV	Site-saturation mutagenesis	5'-ATGCAGCCGCCGGCGTTGATCACAT-3’
AmDH Domain FWD	AA37-168 domain mutagenesis	5'-GCAACGATCCGGCGACAGGACTAAGG-3'
AmDH Domain REV	AA37-168 domain mutagenesis	5'-CGAACGCCTCTTTTGCCGCCGCCTTC-3'
T124C/M130V	Combinatorial mutagenesis	5'-CTTGGCGGCCGTTTCTATACAGGTtgTGATATGGGAACGAATgTGG-3'
T124/M130	Combinatorial mutagenesis	5'-CTTGGCGGCCGTTTCTATACAGGTACTGATATGGGAACGAATATGG-3'
T124C/M130	Combinatorial mutagenesis	5'-

		CTTGGCGGCCGTTTCTATACAGGTtgT GATATGGGAACGAATATGG-3'
T124/M130V	Combinatorial mutagenesis	5'- CTTGGCGGCCGTTTCTATACAGGTAC TGATATGGGAACGAATgTGG-3'
C142Y	Combinatorial mutagenesis	5'- CACGCCATGAAAGAAACAAACTaCAT TGTTGGGGTGCCGGAAGC-3'
C142	Combinatorial mutagenesis	5'- CACGCCATGAAAGAAACAAACTGCA TTGTTGGGGTGCCGGAAGC-3'
N155S/P158L	Combinatorial mutagenesis	5'- GGCTCATCCGGCAgCCCATCGCtGGCG -3'
N155/P158	Combinatorial mutagenesis	5'- CGGCTCATCCGGCAACCCATCGCCGG C-3'
N155S/P158	Combinatorial mutagenesis	5'- GGCTCATCCGGCAgCCCATCGCCGGC- 3'
N155/P158L	Combinatorial mutagenesis	5'- CGGCTCATCCGGCAACCCATCGCtGG CG-3'
Y162H	Combinatorial mutagenesis	5'- GCCcACGGCGTATACCGCGGCATGAA GGCATG-3'
Y162	Combinatorial mutagenesis	5'- CGCCTACGGCGTATACCGCGGCATGA AGGCATG-3'
G177D	Combinatorial mutagenesis	5'- GAGGCGTTCGaCAGCGATTCGCTCGA AGGAAAAGTCGTC-3'
G177	Combinatorial mutagenesis	5'- GAGGCGTTCGGCAGCGATTCGCTCGA AGGAAAAGTCGTC-3'
L146V F	Site-directed mutagenesis	5’-TTGTTGGGGTGCCGGAAGCTTAC-3’

L146V R	Site-directed mutagenesis	5’-CTTCCGGCACCCCAACAATGTAG-3’